LETTERS

Morphology and dynamics of the upper cloud layer of Venus

W. J. Markiewicz[1], D. V. Titov[1,2], S. S. Limaye[3], H. U. Keller[1], N. Ignatiev[2], R. Jaumann[4], N. Thomas[5], H. Michalik[6], R. Moissl[1] & P. Russo[1]

Venus is completely covered by a thick cloud layer, of which the upper part is composed of sulphuric acid and some unknown aerosols[1]. The cloud tops are in fast retrograde rotation (super-rotation), but the factors responsible for this super-rotation are unknown[2]. Here we report observations of Venus with the Venus Monitoring Camera[3] on board the Venus Express spacecraft. We investigate both global and small-scale properties of the clouds, their temporal and latitudinal variations, and derive wind velocities. The southern polar region is highly variable and can change dramatically on timescales as short as one day, perhaps arising from the injection of SO_2 into the mesosphere. The convective cells in the vicinity of the subsolar point are much smaller than previously inferred[4–6], which we interpret as indicating that they are confined to the upper cloud layer, contrary to previous conclusions[7,8], but consistent with more recent study[9].

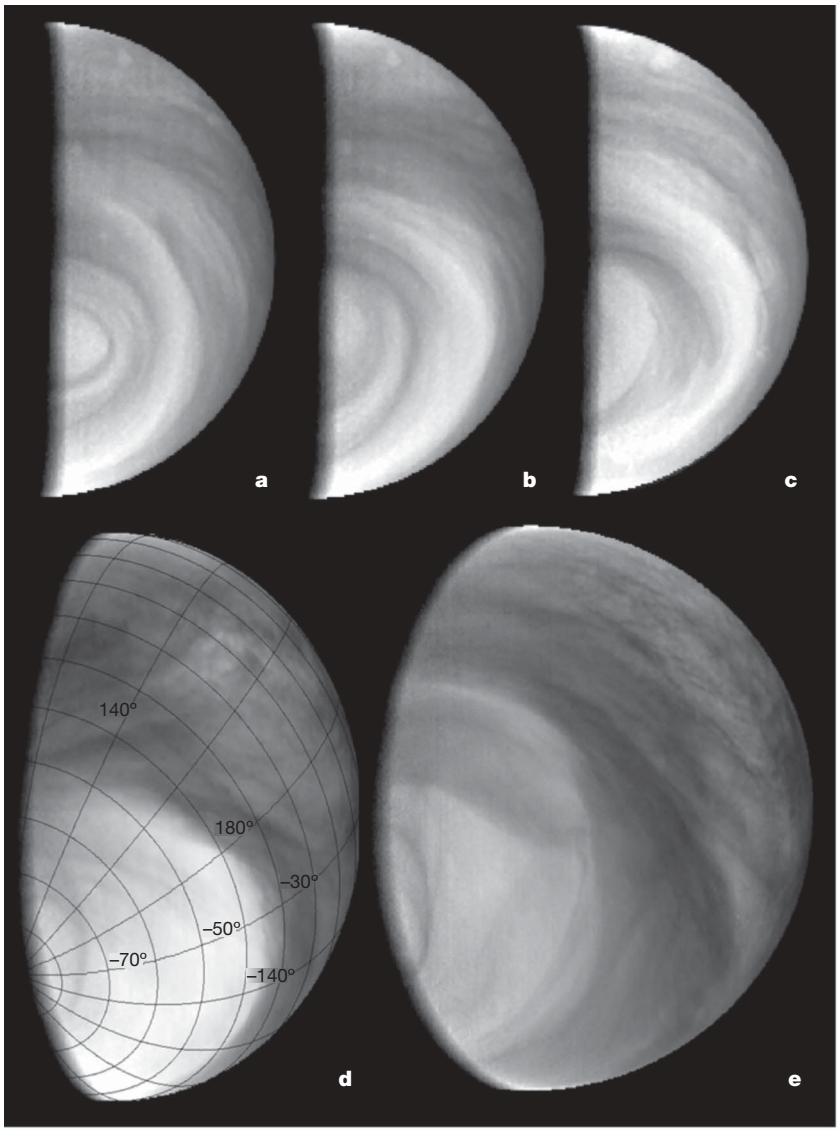

Figure 1 | Variability of the clouds and hazes in the south polar region. On 11 April 2006, the Venus Express spacecraft was inserted into an elliptical polar orbit around Venus with a 24-hour period. The mission aims at a global investigation of the Venus atmosphere by a powerful suite of remote sensing instruments[6], including the VMC, which is a wide-angle digital camera, to investigate the cloud morphology and dynamics of the visible cloud tops. The VMC takes images in four narrow spectral bands—in ultraviolet (365 nm), visible (513 nm) and near-infrared (965 and 1,010 nm)—with spatial resolution from 50 km per pixel down to 200 m per pixel. The ultraviolet channel is centred at the characteristic wavelength of the mysterious ultraviolet absorber, for which the observed contrasts are maximal. This figure shows images of Venus captured by the VMC in the ultraviolet channel. The south pole is at the terminator in the bottom left of the images. Super-rotation is in the anticlockwise direction. All five images are corrected for the solar incidence angle to enhance the near-terminator region. **a**–**c**, These images are from orbits 67 (**a**), 68 (**b**) and 70 (**c**). The period of super-rotation varies between three and five days, depending on the latitude (compare Fig. 2). Strong variability of the near-polar features from day to day is obvious. An extreme case of such variability is shown in **d**: the bright haze located above the absorbing cloud layer expanded to ~35° S, and also became denser, masking all the features except the oval. Temporal variations in the polar regions of Venus were previously observed by the Pioneer Venus Orbiter Cloud Photopolarimeter (OCPP) experiment at various timescales[16]. The timescale of the observed changes over about one day in the appearance of polar region is very short. Panel **e** was obtained from the ascending branch of the orbit, and shows the full view of the southern hemisphere from equator (right) to the pole.

[1]Max-Planck-Institut für Sonnensystemforschung, D-37191 Katlenburg-Lindau, Germany. [2]Space Research Institute (IKI), 117997 Moscow, Russia. [3]Space Science and Engineering Center, University of Wisconsin, Madison, Wisconsin 53706, USA. [4]Institut für Planetenforschung, DLR, 12489 Berlin, Germany. [5]Physikalisches Institut, CH-3012 Bern, Switzerland. [6]IDA, TU Braunschweig, D-38106 Braunschweig, Germany.

The Venus Express orbit provides an opportunity both to image the South pole in nadir geometry and to obtain high-resolution close-up views of the Northern hemisphere. Figure 1 shows global views of the Southern hemisphere taken by the ultraviolet channel of the Venus Monitoring Camera (VMC) from a distance of 60,000–40,000 km. A bright mid-latitude band separates darker low latitudes from the polar regions, in which global streaks indicate atmospheric parcels spiralling towards the pole. The polar vortex, originally discovered at thermal infrared wavelengths[10], is now observed by the VMC as the dark oval ultraviolet feature (Fig. 1a). The cloud pattern at high latitudes very much resembles the structure of terrestrial hurricanes, but the Venus polar vortex is three to four times larger. In the lower latitudes the cloud morphology is mottled, indicating vigorous convection (see below).

We find that the south-polar region is highly variable on short timescales. Figure 1a–c shows images taken in three nearly consecutive orbits. They show significant changes in the polar cloud pattern on timescales of one day or less. The observed variations are manifestations of global atmospheric motions and wave activity or changes in the properties of the bright upper haze. On 13 January 2007 (orbit 267), the VMC observed a dramatic change of this type (Fig. 1d). Over several days, from 9 to 13 January, the brightness of the southern polar region increased by about 30%. The bright polar haze, the boundary of which is usually located at ~55° S, expanded to ~35° S. Dark streaks commonly seen in the polar region almost disappeared, indicating that the total opacity of the haze veil exceeded unity. The polar contrast features began reappearing again one day later.

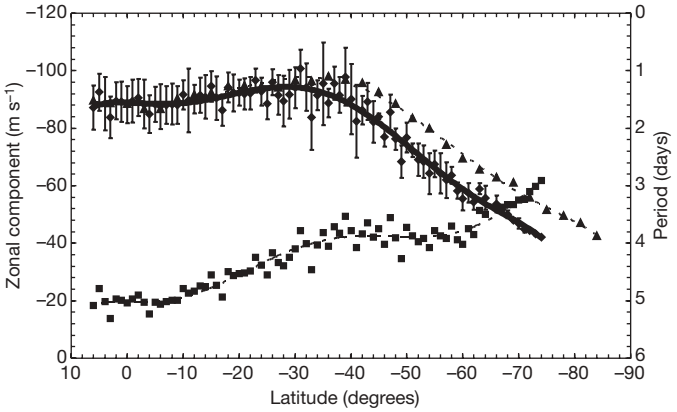

Figure 2 | Wind speeds from tracking cloud features. Latitudinal profile of the east–west component (the negative sign implies the same sense as the rotation of the solid planet) of the cloud motions obtained from digital tracking of features observed by the VMC from orbits 263–267 (solid and dashed curves). The solid curve shows the profile when only the vectors between 11:00 and 13:00 Local Solar Time are averaged, whereas the dashed curve includes all local times measured (~9:00 to 15:00) The rotation period is also shown (right-hand scale, lower, dot-dashed curve). The data points represent averages in one-degree-wide latitude bins and the curves show sixth-degree polynomial fits to the data. The fit equations for the zonal component U (in m s^{-1}) and their regression coefficients R are: $U(11{:}00\text{–}13{:}00\,\mathrm{LST}) = 10^{-8}x^6 + 2\times10^{-6}x^5 + 0.0002x^4 + 0.0041x^3 + 0.022x^2 - 0.0758x - 88.976$; $R^2 = 0.9662$ (diamond symbols; solid line). $U(\mathrm{all\ LST}) = 5\times10^{-9}x^6 + 10^{-6}x^5 + 7\times10^{-5}x^4 + 0.0015x^3 - 0.0121x^2 - 0.1183x - 88.432$; $R^2 = 0.9949$ (triangle symbols; dashed line). The fit equation for the period (in days) and its R value are: $P = -5\times10^{-10}x^6 - 10^{-7}x^5 - 7\times10^{-6}x^4 - 0.0002x^3 - 2\times10^{-6}x^2 + 0.0027x - 5.0148$; $R^2 = 0.9395$ (square symbols; dot-dashed line) Two independent visual tracking estimates were obtained that provide confidence in the wind profile at latitudes between ~10° N and ~−45° S. At higher latitudes the contrast in the ultraviolet images is much reduced and yields far fewer targets for visual tracking. The root-mean-square (r.m.s.) deviation of digital tracking results is typically ~20 m s^{-1}. The vectors were first averaged over each orbit and then averaged together over orbits 263–267. The error bars represent 1 r.m.s. deviation values of the average of the zonal component to each orbit (which in turn is an average of all the points in one-degree-wide latitude bins).The latitude wind profiles show almost constant velocity of 90–100 m s^{-1} at low latitudes in agreement with the earlier measurements. However, above −40° latitude the wind velocity quickly decreases towards the pole. Cyclostrophic balance from thermal structure observations from the Pioneer Venus and Venera missions yields strong mid-latitude jets with wind speeds up to 140 m s^{-1} at ~−55° (refs 14, 17). However, the difference may not be significant, given the different time periods of the observations and the insufficient thermal structure data.

The processes of diffusion growth of sulphuric acid particles, eddy mixing and sedimentation have timescales of a few months at these altitudes and thus do not seem to be relevant[1]. Homogeneous nucleation can lead to quick formation of large amounts of new particles in the submicrometre size range ($r \approx 0.1$ μm), providing the system reaches high values of supersaturation (~10–100). In the case of the Venus upper atmosphere, this implies either abrupt cooling or injection of large amounts of SO_2 molecules in this region. Both mechanisms imply some changes in the dynamical regime of high and mid-latitudes. Subsequent clearing can be explained by the quick decrease of haze opacity due to coagulation, a process that effectively decreases the number of particles and opacity. The coagulation timescale is $t_{coag} \approx 2/Kn$, where n is the number density and K is the coagulation kernel. For the brownian coagulation[1], $K \approx 10^{-9}$ cm^3 s^{-1}. VMC observations of clearing of the polar regions during one day (~10^5 s) indicate that the aerosol number density in the upper haze is $n \approx 10^4$ cm^{-3}. VMC observations show that in the peak of brightening on 13 January the upper haze obscured the cloud top, which implies an opacity of $\tau \approx 1$. We can also estimate the geometrical thickness H of the upper haze layer. The opacity is $\tau \approx \pi r^2 QnH$,

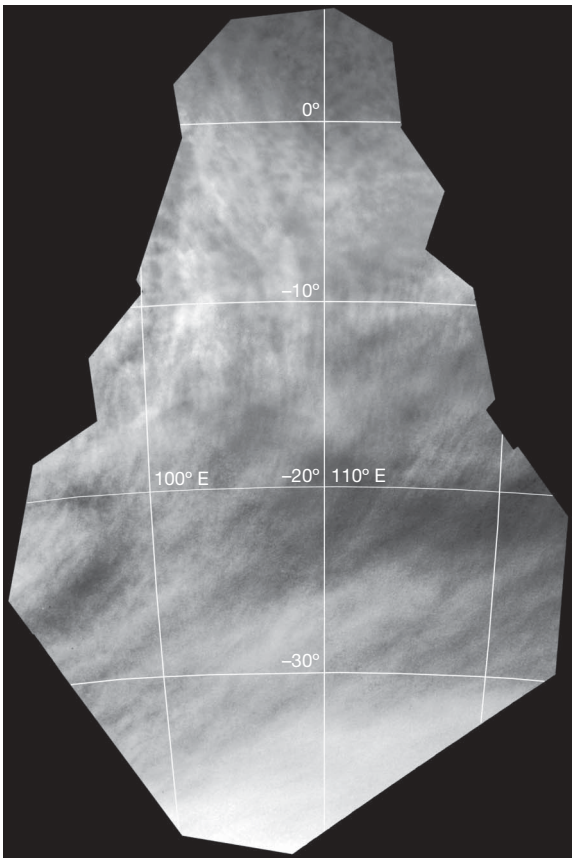

Figure 3 | A mosaic of VMC ultraviolet images showing streaks, wave trains and convection cells (orbit 116). The elongated orbit of Venus Express allows us to zoom into the cloud features while the spacecraft approaches the planet. This mosaic shows that mottled and chaotic cloud patterns at low latitudes give way to approximately zonally oriented streaks at about −15° latitude. This indicates a transition from a dynamical regime that is dominated by local convection at the subsolar point to a quasi-laminar flow.

where $Q \approx 2$ is the extinction efficiency. Assuming other values are as derived above, we obtain $H \approx 2$ km, which seems to be a reasonable value.

Tracking the motions of ultraviolet markings was routinely used in the earlier observations to determine wind velocities at the cloud tops[2,5,11–14] (~70 km). The VMC observations have significant advantages in comparison to the earlier missions. First, the imaging sequences have significant duration (~8 h) and good temporal resolution. Second, the Venus Express orbit allows the VMC to extend wind tracking to middle and high latitudes that were hardly accessible by the earlier missions. Figure 2 shows the preliminary results of zonal winds derived from observations in orbits 263–267.

Because the Venus Express pericentre is kept in the altitude range 250–350 km, the highest spatial resolution is less than 200 m per pixel. Figures 4 and 5 show more detailed images of various regions in Fig. 3. Wave trains, located perpendicular to the direction of cloud streaks, are ubiquitously present at the equatorial edge of the bright polar band and indicate vivid wave activity in this transition region.

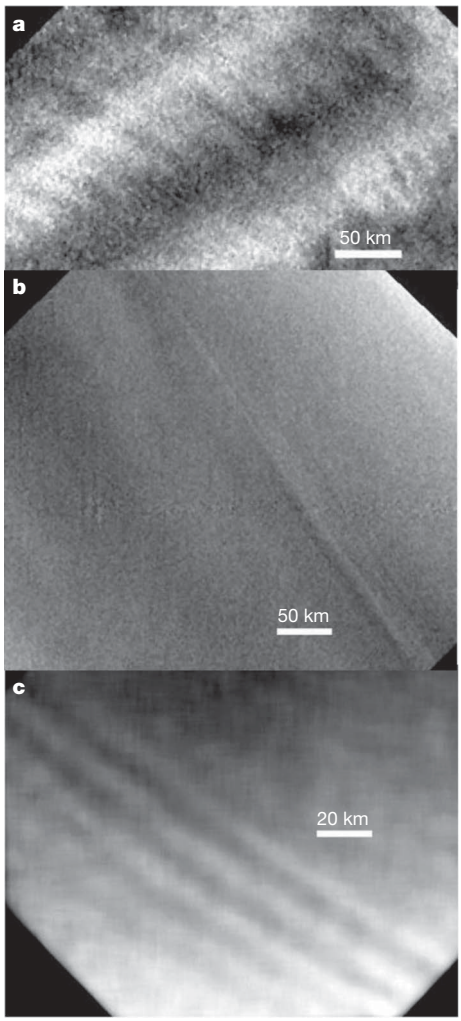

Figure 4 | Three VMC views of Venus clouds with wave-like structures. **a**, An image of a wave train in mid-latitudes at 52° N, −166° E. The typical wavelength of these waves is a few tens of kilometres. **b**, Long linear features such as this one at 54° N, −62° E are occasionally observed, the nature of which is not clear. **c**, A wave train in the polar region (77° N, −51° E). Images **a** and **b** are taken in the ultraviolet channel, and image **c** in the near-infrared. We note that the correlation between the ultraviolet and near-infrared cloud markings that was first evident in Galileo observations[12] frequently appears in the VMC close-up images. This correlation implies that similar mechanisms are responsible for both ultraviolet and near-infrared contrasts and that the unknown ultraviolet absorber absorbs in the near-infrared as well.

Figure 5 shows details of the equatorial region near the subsolar point (local noon). Figure 5a shows what looks like a wave undergoing instability into a more turbulent convection. Figure 5b and c shows more vigorous activity. The morphology of the clouds here is dominated by small-scale cells, but many larger-scale linear features can also be seen. The cellular patterns are believed to be convection cells. They are most prominent in the early afternoon but can also be found near the subsolar point on the morning side. Further from the subsolar point, the patterns return to wavy and streaky morphology even in the equatorial region. The horizontal scale of the convection cells is about 20 km. Because the convection is probably in the upper cloud deck, extending from ~57 to 67 km in altitude, the aspect ratio (diameter/depth) of the cells is about 2. This is five times smaller than the lower limit of aspect ratios reported previously[4–8]. These earlier

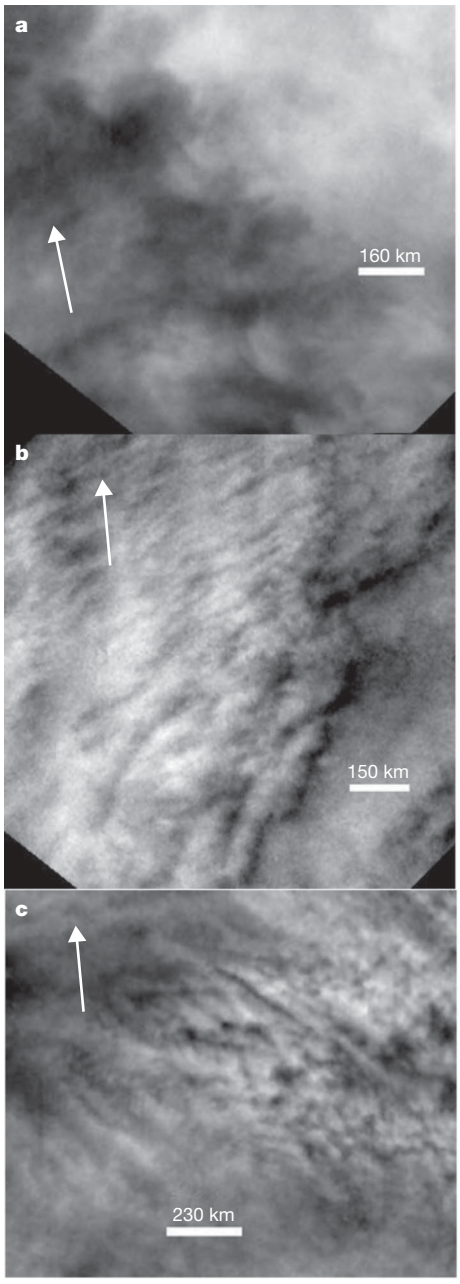

Figure 5 | Three VMC ultraviolet images of the upper cloud deck near the subsolar point. The arrows point to the north. **a**, Wave-like structures transforming into a convective mottled morphology (17° N, −143° E), LST = 14:32. **b**, Streaks and convective cells on the equator (0° N, −150° E), LST = 14:41. **c**, Small convection cells downstream of the subsolar point (10° N, 125° E), LST = 13:16.

estimates were based on data with lower temporal and concurrent spatial resolution than is possible with the VMC. We believe that their inferred convection cells were actually clusters of cells that are now individually resolved—as seen in Fig. 5b, c. Studies of penetrative convection[9,15] have investigated the 40–60 km cloud layer, deeper than the VMC can image, and have relied on the existence of the neutral and stable layers seen in the thermal structure revealed from Pioneer probes and confirmed by Soviet landers. These studies showed that convection may penetrate downward into the stable layer from the neutral layer with aspect ratios of ~100 in the subsolar region. Our observations suggest that the convection in the subsolar region occurs on smaller scales and takes place in the upper reaches of the cloud layer, consistent with more recent study[9]. The subsolar region is where Venus' atmosphere absorbs most of the solar radiation. This energy somehow has to be distributed throughout the planet to drive super-rotation. With deep convection, the transport of energy could be efficiently accomplished dynamically. Our present conclusion—that the convection is shallow—requires a reassessment of radiative energy transport from the subsolar region to the rest of the atmosphere. Further analysis should help in understanding the vertical coupling in the Venus atmosphere and the mechanism of super-rotation.

Received 8 May; accepted 20 September 2007.

1. Esposito, L. W. *et al.* in *Venus* (eds Hunten, D. M., Colin, L., Donahue, T. M. & Moroz, V. I.) 484–564 (Univ. Arizona Press, Tucson, 1983).
2. Limaye, S. S. Venus atmospheric circulation: known and unknown. *J. Geophys. Res.* **112,** E04S09, doi:10.1029/2006JE002814 (2007).
3. Markiewicz, W. J. *et al.* Venus monitoring camera for Venus Express. *Planet. Space Sci.* **55,** 1701–1711 (2007).
4. Murray, B. C. *et al.* Venus: Atmospheric motion and structure from Mariner 10 pictures. *Science* **183,** 1307–1315 (1974).
5. Rossow, W. B. *et al.* Cloud morphology and motions from Pioneer Venus images. *J. Geophys. Res.* **85,** 8107–8128 (1980).
6. Covey, C. C. & Schubert, G. Mesoscale convection in the clouds of Venus. *Nature* **290,** 17–20 (1981).
7. Baker, R. D. II & Schubert, G. Cellular convection in the atmosphere of Venus. *Nature* **355,** 710–712 (1992).
8. Belton, M. J. S. *et al.* Cloud patterns, waves, and convection in the Venus atmosphere. *J. Atmos. Sci.* **33,** 1394–1417 (1976).
9. Baker, R. D., Schubert, G. & Jones, P. W. High Rayleigh number compressible convection in Venus' atmosphere: Penetration, entrainment and turbulence. *J. Geophys. Res.* **104,** 3815–3832 (1999).
10. Taylor, F. W. *et al.* Structure and meteorology of the middle atmosphere of Venus: infrared remote sensing from the Pioneer Orbiter. *J. Geophys. Res.* **85,** 7963–8006 (1980).
11. Rossow, W. B., Del Genio, A. D. & Eichler, T. Cloud tracked winds from Pioneer Venus OCPP images. *J. Atmos. Sci.* **47,** 2053–2084 (1990).
12. Belton, M. J. S. *et al.* Images from Galileo of the Venus cloud deck. *Science* **253,** 1531–1536 (1991).
13. Toigo, A., Gierasch, P. J. & Smith, M. D. High resolution cloud feature tracking on Venus by Galileo. *Icarus* **109,** 318–336 (1994).
14. Newman, M. G., Schubert, G., Kliore, A. J. & Patel, I. R. Zonal winds in the middle atmosphere of Venus from Pioneer Venus radio occultation data. *J. Atmos. Sci.* **41,** 1901–1913 (1984).
15. Baker, R. D., Schubert, G. & Jones, P. W. Cloud-level penetrative compressible convection in the Venus atmosphere. *J. Atmos. Sci.* **55,** 3–18 (1998).
16. Sato, M., Travis, L. D. & Kawabata, K. Photopolarimetry analysis of the Venus atmosphere in the polar regions. *Icarus* **124,** 596–585 (1996).
17. Zasova, L. V. Ignatiev, N. Khatuntsev, I. & Linkin, V. Structure of the Venus atmosphere. *Planet. Space Sci.* **55,** 1712–1728 (2007).

Acknowledgements S.S.L. was supported by a NASA grant.

Author Information Reprints and permissions information is available at www.nature.com/reprints. Correspondence and requests for materials should be addressed to W.J.M. (markiewicz@mps.mpg.de).